



RESEARCH ARTICLE

Substitutability research for forward-scatter meters in indoor low-visibility environments

Zibo Zhuang¹  | Jinfeng Li¹ | Pak Wai Chan²  | Hongda Tai¹

¹Flight Academy of CAUC, Civil Aviation University of China, Tianjin, China

²Aviation Weather Services, Hong Kong Observatory, Hong Kong, China

Correspondence

Hongda Tai, Flight Academy of CAUC, Civil Aviation University of China, Tianjin 300300, China.
Email: hdtai@cauc.edu.cn

Funding information

Central Foundation of University of China, Grant/Award Number: 3122018F008; National Natural Science Foundation of China, Grant/Award Numbers: 41905129, 42075008, U1933103, U2033207

Abstract

Visibility is a crucial parameter for aeronautical operations. Forward-scatter meters are recommended to measure it because of inherent advantages. With wide use at airports, the substitutability among forward-scatter meters is worth paying attention to, especially in low-visibility environments. To confirm the substitutability among forward-scatter meters, eight kinds of forward-scatter meters were installed in an indoor atmospheric environment simulation chamber. The observed values of each of the eight forward-scatter meters in haze and smoke low-visibility environments were collected. By least-squares fitting analysis and the ATE/LER zones method, in the haze, the two sets of CS125 can be substituted for each other in visibilities lower than 2000 m. PWD20 and V30 can be substituted for each other at visibilities lower than approximately 1200 m. From 1200 to 2000 m, the consistency of the two instruments is poor. In the smoke, CS125 and PWD20 display good substitutability with each other when visibility is less than 2000 m. If only focusing on visibilities less than approximately 1000 m, the VPF-710 and V30 instruments can be substituted with each other.

KEYWORDS

forward-scatter meters, low visibility, substitutability

1 | INTRODUCTION

Visibility is a basic meteorological factor that not only refers to the transparency of air but also closely relates to transportation, especially civil aviation. Airport opening, precision approach and landing operations are all related to visibility. Low visibility below the approved minimum aircraft and flight certification can prevent aircraft from utilizing a runway (ICAO, 2011).

Objectively, visibility can be calculated from the extinction coefficient measured by instruments and

represented by Meteorological Optical Range (MOR). A variety of instruments are available to obtain MOR, but at present, only those based on transmissometers and forward-scatter meters are recommended (ICAO, 2005). In the two types endorsed by the International Civil Aviation Organization (ICAO), forward-scatter meters have certain advantages over transmissometers, such as ease of installation, little maintenance, low expense and relative calibration at any time. Precisely because of these, forward-scatter meters have been popularized to gradually replace traditional transmissometers. However,

This is an open access article under the terms of the Creative Commons Attribution-NonCommercial-NoDerivs License, which permits use and distribution in any medium, provided the original work is properly cited, the use is non-commercial and no modifications or adaptations are made.

© 2022 The Authors. *Meteorological Applications* published by John Wiley & Sons Ltd on behalf of Royal Meteorological Society.

a scatter meter operates on the opposite principle from the transmissometer (Schwartz & Burnham, 1987). To evaluate the accuracy of forward-scatter meters or select a suitable forward-scatter meter to replace the original transmissometer, a series of comparative tests of the two types were conducted either outdoors or indoors. These tests are normally conducted in the field, such as an evaluation during a 17-month period at Otis Air National Guard Base (Schwartz & Burnham, 1987), a field test beginning in fall of 2006 lasting 9 months in Germany (Waas, 2008) and a field study from November 2010 to April 2013 at Hong Kong International Airport (Chan, 2016). Due to the uncertainty of natural weather conditions, the comparative period is always long, and a large amount of uninteresting data can be easily collected. A large climate chamber was used to examine the feasibility of visibility sensors with a twofold goal of (1) examining visibilities lower than commonly experienced in nature and (2) accelerating the evaluation process (Burnham, 1983). In addition, because of the steady weather conditions in the indoor chamber, the calibration of forward-scatter meters has been carried out indoors (Chong et al., 2020). However, not all sensors available on the market perform equally accurately; in fact, there may be significant differences in performance (ICAO, 2011). Even a transmissometer has a few inherent sources of error (ICAO, 2005). No standard test methods or measurement practices are available for visibility (Crosby, 2003). Research on the substitution of visibility instruments is of significance to practical applications. First, there is a real need to replace the original visibility instrument at airports. Second, new instruments are deployed operationally to introduce apparent changes in site climatology, and observations from new instruments should be compared over an extended interval before the old measurement system is taken out of service (WMO, 2018).

With the wide use of forward-scatter meters at airports, substitutability among them is worth paying attention to. To clarify the differences and evaluate substitutability among them, eight kinds of forward-scatter meters were installed in an indoor atmospheric environmental simulation chamber. The whole experimental process and analysis results are discussed below.

2 | TEST INSTRUMENTS AND EXPERIMENTAL PROCESS

2.1 | Test instruments

The eight kinds of forward-scatter meters we selected have been widely used at airports. To shorten the

experimental period and obtain more continuous low-visibility observations, all the test instruments were installed in an indoor atmospheric environmental simulation chamber. The position of each forward-scatter meter is random, but the sampling volume must be in the same comparably homogeneous space. The homogeneous space in the chamber is discussed in Section 2.2. The eight kinds of instruments include VPF-730, VPF-710, Model 6400, V30, PWD20, PWS100 and the two sets of CS125. One CS125 was named CS125-1 and the other was named CS125-2. Brief descriptions of the eight instruments are given below.

VPF-730—VPF-730 not only measures visibility but also identifies precipitation. The unique backscatter receiver gives the ability to distinguish frozen from liquid precipitation. To avoid the influence of bright or flashing lights, the VPF-730 transmitter emits 850 nm, 2 kHz modulated infrared light sources combined with narrow pass band optical filters and synchronous detection at the receiver. Its forward scattering angle covers a range of 39–51°, centred at 45°. The measurement range goes from 10 m to 75 km, and the measurement accuracy is $\pm 2\%$ at 2 km, $\pm 10\%$ at 16 km and $\pm 20\%$ from 16 to 30 km.

VPF-710—VPF-710 and VPF-730 belong to the VPF series of forward-scatter meters produced by Biral. They have the same basic opto-mechanical and electronic components. However, unlike VPF-730, VPF-710 is only a visibility instrument with no precipitation recognition capability.

Model 6400—Model 6400 can output visibility and extinction coefficients. Its transmitter emits an infrared 880 nm wavelength light beam into the sample volume at a 42° scattering angle. The modulation of the light source is also used to suppress background noise and light intensity variation. The visibility conditions are monitored over a range of 6 m–80 km, with an accuracy of $\pm 10\%$.

V30—It is also known as DNQ4, which has been used in the South China Sea. Infrared light at 850 nm is emitted from transmitters. The measurement range of the instrument ranges from 10 m to 30 km with an accuracy of $\pm 10\%$ in visibility up to 10 km and $\pm 20\%$ from 10 km to 30 km.

PWD20—PWD20 is one of the Vaisala PWD series sensors, with a measurement range of 10 m–20 km, an accuracy of $\pm 10\%$ from 10 m to 10 km and $\pm 15\%$ above 10 km. Near-infrared light with an 875 nm wavelength is emitted at a 45° scattering angle.

PWS100—The PWS100 instrument is a laser-based sensor capable of determining precipitation. A near-infrared light-emitting diode with a peak wavelength of 830 nm is used, and the modulation frequency is 96 kHz. Its visibility measurement range covers up to 20 km, with an accuracy of $\pm 10\%$ up to 10 km. Unlike the other

forward-scatter meters, PWS100 consists of a laser head and two sensor heads: one of the sensor heads is at a 20° angle from the laser unit axis in the horizontal plane, and the other one is at the same angle in the vertical plane.

CS125—Similar to VPF-730 and PWS100, CS125 also had the ability to identify precipitation. CS125 can report visibility from 5 m to 75 km, with an accuracy of $\pm 8\%$ in visibilities up to 600 m, $\pm 10\%$ up to 10 km, $\pm 15\%$ up to 15 km and $\pm 20\%$ above. The emitter produces a beam of near-infrared light with a central wavelength of 850 nm and a modulation frequency of 1 kHz. The forward scattering angle is 42°.

2.2 | Experimental process

To perform substitutability research for the eight kinds of forward-scatter meters, it is necessary to collect observed values of each instrument, especially in a low-visibility environment, which has a considerable impact on civil aviation. Due to unpredicted natural weather conditions, an indoor atmospheric environmental simulation chamber was used. The indoor simulation chamber was built with hardened glass and dimensions of $1.8 \times 1.6 \times 55.7 \text{ m}^3$. To prevent the influence of external light interference and glass effects on reflection and scattering of the emitted light by the instruments, black shading cloths were added to the outside and inside of the chamber. In addition to the infrastructure, the subsystems, including power supply, gas supply and circulation, drainage, monitoring and water supply, are all in normal condition.

Before the experiments, all calibrated forward-scatter meters should be installed in the chamber. It should be noted that only instruments in homogeneous space are comparable, and the data analysis must be conducted only during “homogeneous” events (ICAO, 2005). Therefore, the sampling volume of each forward-scatter meter in the chamber must be within the same comparably homogeneous space. To find the space, by CFD simulation software, we modelled the chamber using Gambit, and the particle trajectories were calculated by using the N-S equation of Fluent. For parameter settings, the particle diameter is $1 \mu\text{m}$, the injection rate is $0.1 \text{ m}^3/\text{min}$ and the particle concentration is $10^8 \text{ Particles}/\text{cm}^3$. Through the simulation results, the coordinates of the relatively homogeneous space in the chamber are shown in Equation (1):

$$\begin{cases} x = 0.4 \sim 1.2 \text{ m} \\ y = 2.5 + n \times 5 (n = 0, 1, 2, \dots, 10) \text{ m} \\ z = 0.7 \sim 1.1 \text{ m} \end{cases} \quad (1)$$

where n is a position every 5 m. However, the consistency of the results between the software simulation and experiment is the key aspect to verify homogeneity. To do this, a baseline changing visibility measurement system was conducted in the chamber (Hongda et al., 2017). The system was composed of a fixed transmitter and a mobile receiver that moved from 0 m to 55 m in the chamber at a speed of 0.4 m/s, stopped every 5 m and remained motionless for 3 s to measure and record transmittance. The receiver moved to 55 m and back twice to obtain four measured values at each measurement point. According to the Beer–Lambert law, given as follows Equation (2):

$$\tau(R_i) = e^{-\sigma_i R_i} (i = 1, 2, 3, \dots, n) \quad (2)$$

where $\tau(R_i)$ is the transmittance measured by the baseline changing system and R_i is the baseline between the transmitter and receiver. The extinction coefficient σ_i of every measurement point could be calculated by taking the logarithm of both sides of the above formula. To return the precise extinction coefficient, the total least-squares method was used to fit the extinction coefficient array (Equation (3)).

$$[(R_1, \ln \tau_1), (R_2, \ln \tau_2), \dots, (R_n, \ln \tau_n)] \Rightarrow [\sigma_1, \sigma_2, \dots, \sigma_n] \quad (3)$$

The coefficient of determination can be used to evaluate the effect of the fitting (Rao et al., 1973). The closer the coefficient of determination is to 1, the better the fit of the total points and the smaller the difference between each measurement point's extinction coefficient. When the visibility is lower than 2000 metres, the coefficient of determination is greater than 0.96 and is greater than 0.98 in visibilities lower than 1000 metres. The consistency of the longitudinal distribution of the extinction coefficient proved the relative uniformity of the chamber. All instruments' sampling volumes were placed at the same uniform height along the longitudinal homogeneous space.

To create the experimental environment, initially, a large axial-flow fan with 10 pairs of horizontal fans renewed the indoor air to eliminate the influence of impurities. Saturated ammonium sulphate solution was used as the experimental material to simulate haze. China suffers from serious haze pollution characterized by extremely low visibility caused by a high loading of fine particulate matter (PM_{2.5}) (Li et al., 2019). For PM_{2.5} chemical components, NH_4^+ , NO_3^- and SO_4^{2-} became the main pollutants (Xunrui et al., 2021). Ammonium sulphate has a major extinction contribution (Han et al., 2012; Tao et al., 2009). The saturated ammonium sulphate solution was converted by the aerosol generator ATM-241 into the corresponding fine saline aerosols (mainly smaller than

1 μm). The produced fine saline aerosols were sprayed into the chamber by aerosol inlets. Based on uniformity requirements, certain parameters need to be controlled for the aerosol inlets. The particle injection rate of the inlets is 0.1 m^3/min , and the particle concentration is 10^8 Particles/ cm^3 . In addition, 10 pairs of horizontal fans with 2500 r/min speed that produced 12 m^3/min air flow were constantly running to mix aerosol particles homogeneously. From December 10 to December 11, the two pieces of Cavendish were used to simulate a low-visibility environment full of smoke.

When the observed values recorded by all instruments decreased to minima and stabilized, the readings of instruments were officially recorded until the observed values of all instruments reached 2000 metres; notably, visibilities greater than 2000 m basically had little effect on civil aviation operational decisions. Considering the difference in the minimum measurement range of each instrument, we mainly focus on the substitution among instruments for visibilities from 50 to 2000 m.

2.3 | Analysis method

All control commands were sent by the server in the observation and control room. The measurement data of the receiver were transmitted to the server by a WLAN. To obtain more observed values for analysis, one-minute averages were collected. The 454 observed values of the eight instruments in visibility up to 2000 m in the haze and 172 observed values in the smoke. The observed values of PWS100 display no upward trend with improved visibility after an initial decline in the haze. The observations of PWS100 were excluded from further analysis. To verify the substitutability among test instruments, the ATE/LER zones method was used in the research.

The ATE/LER zones method, which is also known as the Allowable Total Error and Limits for Erroneous Results zones method, is encouraged by the Food and Drug Administration (FDA) to assess the agreement between two methods (Karaźniewicz-Łada et al., 2014). If the two methods have complete agreement, the values of the two would lie on the equal line, but the values always fluctuate around the line because of differences. Before beginning the consistency study, performance criteria should be established. With the established performance criteria, the ATE/LER zones are divided into two main zones, namely, the ATE zones and LER zones. The observations between the two methods should span the measuring range and adequately represent all possible values of the one method on x-axis consistent with the measuring range of the other method on y-axis. According to

observations of the one method on x-axis, the observations should divide into low, medium and high relevant intervals with approximately the same number in each. For each interval, the percentage of the observations that fall into ATE zones should approach 95%, and no observations fall into LER zones. Furthermore, the percentage of the observations over the entire measuring range that fall within ATE zones with a lower one-sided 95% confidence bound should exceed 92%, and that fall within LER zones with an upper one-sided 95% confidence bound should be below 1% (FDA, 2008). Consistency between methods must meet the requirements. If two methods show good consistency, we can replace the old method with the new method or use the two interchangeably (Zhou et al., 2011). In addition, for the ATE zones and LER zones, the one-sided 95% confidence bound can be estimated by the Newcombe-Wilson score method, as shown below Equation (4), n is the total sample size, p is the proportion of the values falling within ATE or LER zones, q is $1 - p$ and Z is a unilateral value of $\alpha = 0.05$, which is 1.645.

$$\left[2np + Z^2 \pm Z\sqrt{(Z^2 + 4npq)} \right] / 2(n + Z^2) \quad (4)$$

According to ICAO, the accuracy requirements for MOR are ± 50 m when visibility reaches 500 m, $\pm 10\%$ ranges from 500 m to 2000 m and $\pm 20\%$ above. For visibilities from 50 to 2000 m, the corresponding accuracy requirements are to be used as the acceptable criteria and $\pm 20\%$ as the unacceptable criteria. The ATE/LER zones diagram of the two instruments is shown in Figure 1. If the percentage of values and the one-sided confidence bound meet the requirements of the ATE/LER zones

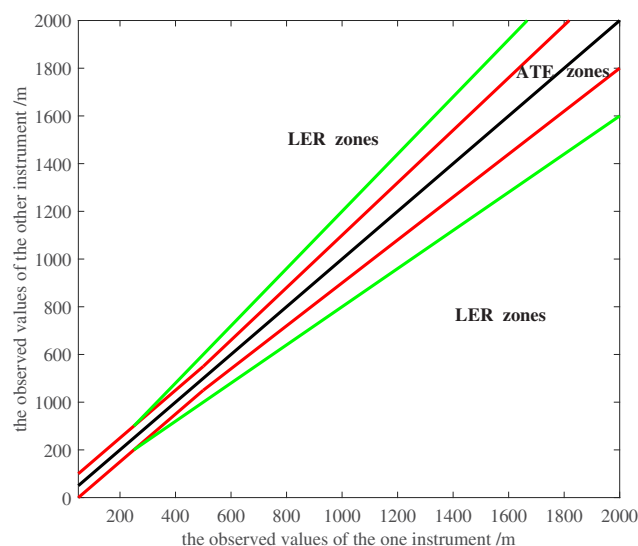


FIGURE 1 The ATE/LER zones diagram of instruments

method, the instrument on the x-axis can be substituted by the instrument on the y-axis.

3 | RESULTS

For the preliminary determination of the substitutability between test instruments, least-squares fitting is performed to obtain the slope. There was a significant correlation between them (correlation coefficient above 0.99 and $p < 0.01$) not only in the haze but also in the smoke. The slope indicates the ratio of the responses of the two instruments over that range; if the two sensors have completely identical responses, the points will all lie on a straight line at a 45° angle (Schwartz & Burnham, 1987), which is almost impossible in most cases. Based on the maximum accuracy requirement being less than 20%, the slope of the two instruments with good consistency should be between 0.8 and 1.2. From the fitting results shown in Tables 1 and 2, regardless of haze or smoke, Model 6400 has higher measurements. Except for Model 6400 and VPF-710 in the haze, all the instruments meet the slope requirement with one or more other instruments. However, simple correlation analysis is insensitive

to systematic error (Zhou et al., 2011), and the ATE/LER zones method should be used for further analysis.

In the haze, for CS125-1, consistency was preliminarily confirmed with CS125-2 and with PWD20. However, based on the ATE/LER zones method and the corresponding diagram shown in Figure 2a, several values of CS125-1 and PWD20 fall into LER zones. As long as the values fall within the LER zones, the consistency between the two instruments is unacceptable according to the requirements. A similar result occurred between V30 and VPF-730 (as shown in Figure 2c,e) and PWD20 with CS125-2 (as shown in Figure 2d); consistency is rejected because of outliers within LER zones. The consistency between CS125-1 and CS125-2 is great, as shown in Figure 2a,b. All values fall into ATE zones we accept in visibilities within 2000 metres. By calculating using Equation (4), the lower one-sided 95% confidence bounds are 99.4% and 99.41%, respectively, which are greater than 92%, and the upper one-sided 95% confidence bounds are 0.6%, which are lower than 1%. The substitutability between the two CS125 is confirmed in the haze. For PWD20 and V30 (as shown in Figure 2c,d), although none fall into the unacceptable LER zones, the percentage of values falling within ATE zones is less than 95% in visibilities from 830 to 2000 m. At

TABLE 1 The slope between the observed values of each test instrument in the haze

x	y						
	CS125-1	CS125-2	V30	PWD20	Model6400	VPF-730	VPF-710
CS125-1		0.9437	1.322	1.147	2.683	1.551	1.976
CS125-2	1.059		1.4	1.215	2.842	1.643	2.093
V30	0.7543	0.7116		0.8666	2.029	1.172	1.494
PWD20	0.8702	0.8213	1.153		2.339	1.352	1.722
Model6400	0.3718	0.3508	0.4927	0.4271		0.5777	0.7362
VPF-730	0.6432	0.6069	0.8515	0.7385	1.729		1.274
VPF-710	0.505	0.4765	0.6688	0.5798	1.357	0.7848	

TABLE 2 The slope between observed values of each test instrument in the smoke

x	y						
	CS125	PWS100	V30	PWD20	Model6400	VPF-730	VPF-710
CS125		1.143	0.9105	0.9421	1.402	0.8752	1.055
PWS100	0.8718		0.7928	0.8224	1.221	0.7611	0.9176
V30	1.094	1.249		1.03	1.538	0.9667	1.163
PWD20	1.061	1.214	0.9653		1.487	0.9275	1.118
Model6400	0.7111	0.8123	0.6495	0.6699		0.6272	0.7549
VPF-730	1.115	1.271	1.025	1.049	1.575		1.199
VPF-710	0.9335	1.065	0.8565	0.8787	1.317	0.8329	

visibilities lower than approximately 1200 m, the values falling into the ATE zones between them are 97.32% and 99.69%, the calculated lower one-sided 95% confidence bounds are 95.45% and 98.62% and the upper one-sided 95% confidence bounds in LER zones are 0.8% and 0.84%, respectively. If only focusing on visibilities lower than

approximately 1200 metres, the two instruments can be substituted with each other. In addition, when PWD20 is substituted with CS125-1, as shown in Figure 2d, only 58% of the values fall into the ATE zones when the observed values of PWD20 are below 2000 m, and PWD20 cannot be substituted with CS125-1. Therefore, in the haze, the two

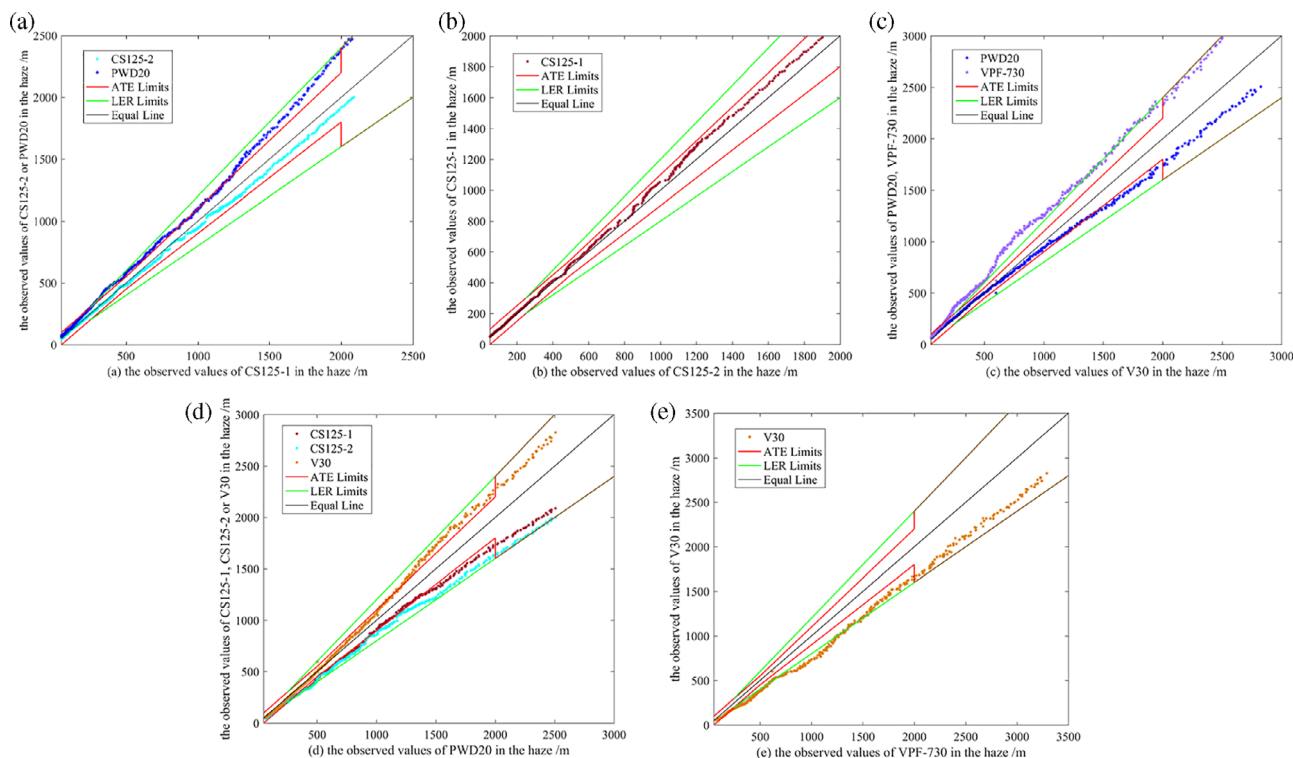


FIGURE 2 (a) ATE/LER zones diagram of CS125-1 with CS125-2 or PWD20 in the haze; (b) CS125-2 with CS125-1; (c) V30 with PWD20 or VPF-730; (d) PWD20 with CS125-1, CS125-2 or V30; (e) VPF-730 with V30

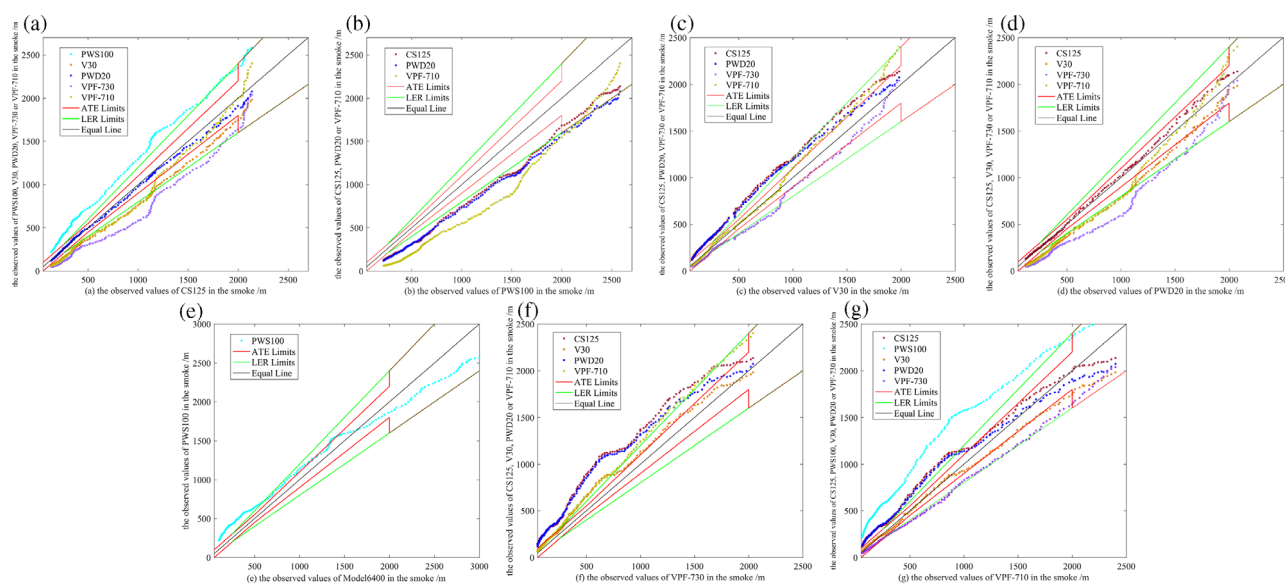


FIGURE 3 (a) ATE/LER zones diagram of CS125 with PWS100, V30, PWD20, VPF-730 or VPF-710 in the smoke; (b) PWS100 with CS125, PWD20 or VPF-710; (c) V30 with CS125, PWD20, VPF-730 or VPF-710; (d) PWD20 with CS125, V30, VPF-730 or VPF-710; (e) model 6400 with PWS100; (f) VPF-730 with CS125, V30, PWD20 or VPF-710; (g) VPF-710 with CS125, PWS100, V30, PWD20 or VPF-730

sets of CS125 can substitute each other at visibilities lower than 2000 metres, and PWD20 and V30 can substitute at visibilities lower than approximately 1200 m.

In the smoke, between all instruments, there is a distinct linear relationship, and most slopes are between 0.8 and 1.2. Similarly, good linearity does not mean consistency. Except for Model 6400, between CS125 and the other instruments, all have acceptable linearity. However, only the values of CS125 with PWD20 all fall into the acceptable zones, as shown in Figure 3a, and with the others, several values fall into LER zones. In addition, as shown in Figure 3d, only CS125 meets the consistency requirements among several preliminary potential replacements for PWD20. The values between PWD20 and CS125 all fall within ATE limits in visibilities lower than 2000 metres, the calculated lower one-sided 95% confidence bounds are all beyond 99% and the upper one-sided 95% confidence bounds are below 1%. It is reasonable to conclude that PWD20 and CS125 are substituted with each other in visibilities below 2000 m. Between the other instruments, most of them have some values falling into LER zones, except the values of VPF-710 with V30 (as shown in Figure 3c,g), although none fall into LER zones when VPF-710 measured visibility below 2000 m, less than 95% of values fall within ATE limits in visibilities from 820 to 2000 m. If only focusing on visibilities lower than approximately 1000 m, the two instruments can be substituted with each other.

4 | DISCUSSION AND CONCLUSION

The substitution of eight forward-scatter meters was considered. To shorten the experimental period and collect more low-visibility observations, an indoor atmospheric environment simulation chamber was used. Compared with field tests, indoor experiments are more convenient to simulate low-visibility weather conditions in a short time. Compared with the previous indoor experiments, a baseline changing system was constructed to check the uniformity of the chamber to avoid systematic error by using different instruments. For the values of linear continuous changes in indoor experiments, the ATE/LER zones method makes it easier to show a trend of changes and differences over all low-visibility measurements. The reliability of the current sample conclusion is evaluated by calculating the 95% confidence bound.

Based on the preliminary analysis by least-squares fitting and the ATE/LER zones method, substitutability is identified among the eight kinds of instruments in the low-visibility environments we created in the chamber. In the haze, the observed values of the two sets of CS125

are highly consistent in visibilities lower than 2000 metres, and it is natural to conclude that they can be substituted for each other. At visibilities lower than approximately 1200 metres, PWD20 and V30 can be substituted with each other. At visibilities from 1200 to 2000 m, the consistency of the two instruments is poor. In the smoke, the values of CS125 and PWD20 display good consistency over the whole measurement range. If only focusing on visibilities lower than approximately 1000 m, VPF-710 and V30 can be substituted with each other. In general, differences in observations do exist between different forward-scatter meters. However, the differences between them can be acceptable and the substitutability between them can be determined in typical conditions, including the range of visibilities and weather conditions.

Although the substitutability of forward-scatter meters is studied in the indoor chamber under haze and smoke, low visibility can be caused by a variety of atmospheric conditions, including heavy rain, blowing snow and so on (Leung et al., 2020). The results for the other kinds of low-visibility weather conditions beyond those considered in the study should be analysed.

ACKNOWLEDGEMENTS

This work was supported by the National Science Foundation of China (Nos. 41905129, U1933103, U2033207 and 42075008) and Central Foundation of University of China (No. 3122018F008).

AUTHOR CONTRIBUTIONS

Zibo Zhuang: Formal analysis (lead); funding acquisition (equal); methodology (lead); writing – original draft (lead); writing – review and editing (lead). **Jinfeng Li:** Data curation (lead); methodology (supporting); visualization (lead); writing – original draft (equal); writing – review and editing (equal). **Pak Wai Chan:** Funding acquisition (equal); project administration (lead); supervision (lead); writing – original draft (equal); writing – review and editing (equal). **Hongda Tai:** Conceptualization (lead); funding acquisition (equal); investigation (lead); resources (lead); validation (lead); writing – original draft (equal); writing – review and editing (equal).

ORCID

Zibo Zhuang  <https://orcid.org/0000-0002-6056-564X>

Pak Wai Chan  <https://orcid.org/0000-0003-2289-0609>

REFERENCES

- Burnham, D.C. (1983) *Evaluation of visibility sensor at the Eglin air Force Base climate chamber*. Report. DOT-TSC-FAA-83-01. Cambridge, MA 02142: Vlope Nation Transportation System Center.

- Chan, P.W. (2016) A test of visibility sensors at Hong Kong international airport. *Weather*, 71(10), 241–246. <https://doi.org/10.1002/wea.2772>
- Chong, W., Bian, Z., Chu, J., He, X. & Jiang, D. (2020) A method for calibrating forward scatter meters indoors. *Metrologia*, 57(6), 065030. <https://doi.org/10.1088/1681-7575/ab993e>
- Crosby, J.D. (2003) *Visibility sensor accuracy: what's realistic?. 12th symposium on meteorological observations & instrumentation*. Long Beach: American Meteorological Society, pp. 1–5.
- Food and Drug Administration Staff (FDA) (2008) Recommendations for Clinical Laboratory Improvement Amendments of 1988 (CLIA) Waiver Applications for Manufacturers of In Vitro Diagnostic Devices.
- Han, S., Bian, H., Zhang, Y., Jianhui, W., Wang, Y., Tie, X. et al. (2012) Effect of aerosols on visibility and radiation in Tianjin, China. *Aerosol and Air Quality Research*, 12, 607–623.
- Hongda, T., Zibo, Z., Lihui, J. & Dongsong, S. (2017) Visibility measurement in an atmospheric environment simulation chamber. *Current Optics and Photonics*, 1(3), 186–195. <https://doi.org/10.3807/COPP.2017.1.3.186>
- International Civil Aviation Organization. (2005) Manual of runway visual range observing and reporting practices. *ICAO Doc*, 9328, 1-1-H-1.
- International Civil Aviation Organization. (2011) Manual on automatic meteorological observing Systems at Aerodromes. *ICAO Doc*, 9837, 1-1-C-1.
- Karaźniewicz-Łada, M., Danielak, D. & Głowska, F. (2014) HPCE and HPLC methods for determination of clopidogrel and its carboxylic acid metabolite in biological samples: a comparative analysis. *Journal of Liquid Chromatography & Related Technologies*, 37(5), 620–623. <https://doi.org/10.1080/10826076.2012.758133>
- Leung, A.C.W., Gough, W.A. & Butler, K.A. (2020) Changes in fog, ice fog, and low visibility in the Hudson bay region: impacts on aviation. *Atmosphere*, 11(2), 186. <https://doi.org/10.3390/atmos11020186>
- Rao, B.R., Mazumdar, S., Waller, J.H. & Li, C.C. (1973) Correction between the numbers of two types of children in a family. *Biometrics*, 29(2), 271–279. <https://doi.org/10.2307/2529391>
- Schwartz, D. and Burnham D. (1987) Otis ANGB Visibility Sensor Field Test Study. Report. AFGL-TR-86-0011, Cambridge, MA 02142.
- Tao, J., Ho, K.-F., Chen, L., Zhu, L., Han, J. & Xu, Z. (2009) Effect of chemical composition of PM_{2.5} on visibility in Guangzhou, China, 2007 spring. *Particuology*, 7(1), 68–75. <https://doi.org/10.1016/j.partic.2008.11.002>
- Waas, S. (2008) Field test of forward scatter visibility sensors at German airports. In: *WMO technical conference on meteorological and environmental instruments and methods of observation (TECO-2008)*. St. Petersburg: World Meteorological Organization.
- WMO (2018) Guide to Instruments and Methods of Observation (No.8). Volume I – Measurement of Meteorological Variables.
- Xun Li, Lin Huang, Jingyi Li, Zhihao Shi, Yiyi Wang et.al. (2019) Source contributions to poor atmospheric visibility in China. *Resources, Conservation and Recycling*, 143, pp:167–177. <https://doi.org/10.1016/j.resconrec.2018.12.029>
- Xunrui, W., Zhang, X., Li, A.n. et al. (2021) Comparative research on visibility and light extinction of PM_{2.5} components during 2014–17 in the North China plain. *Atmospheric and Oceanic Science Letters*, 14(02), 69–75. <https://doi.org/10.1016/j.aosl.2021.100034>
- Zhou, Y., Zang, J., Wu, M., Xu, J. & He, J. (2011) Allowable total error and limits for erroneous results (ATE/LER) zones for agreement measurement. *Journal of Clinical Laboratory Analysis*, 25(2), 83–89. <https://doi.org/10.1002/jcla.20437>

How to cite this article: Zhuang, Z., Li, J., Chan, P. W., & Tai, H. (2022). Substitutability research for forward-scatter meters in indoor low-visibility environments. *Meteorological Applications*, 29(2), e2050. <https://doi.org/10.1002/met.2050>